JOURNAL OF AIRCRAFT
Vol. 30, No. 1, Jan.–Feb. 1993

Engineering Notes

ENGINEERING NOTES are short manuscripts describing new developments or important results of a preliminary nature. These Notes cannot exceed 6 manuscript pages and 3 figures; a page of text may be substituted for a figure and vice versa. After informal review by the editors, they may be published within a few months of the date of receipt. Style requirements are the same as for regular contributions (see inside back cover).

Fastest Climb of a Turbojet Aircraft

Shiva Kumar Ojha*
Indian Institute of Technology, Powai, Bombay-400076, India

Nomenclature

C = thrust specific fuel consumption
C_{D0} = zero-lift drag coefficient
D = drag force on aircraft
E = L/D, aerodynamic efficiency of aircraft
h = altitude
K = induced drag factor
L = lift force on aircraft
R/C = rate of climb
S = wing planform area
T = thrust required
t = endurance, time taken in climb
V = airspeed
W = all up weight of aircraft
x = range, horizontal distance traveled in climb
β = 9296 m in troposphere, and β is 7254 m in stratosphere
Γ = defined by Eq. (9)
γ = climb angle
ζ = $(W_1 - W_2)/W_1$, climb-fuel weight fraction
ρ = density of atmospheric air
σ = ρ/ρ_{SSL}, density ratio

Subscripts
FC = fastest climb
m = maximum
SSL = standard day sea level condition
1 = beginning of climb
2 = end of climb

Introduction

THE fastest climb has maximum rate of climb and takes minimum time to climb. The analytical expressions of airspeed, climb angle, and the rate of climb for the fastest climb have been recently obtained by Hale.[1] This note improves the analysis of Hale by obtaining analytical expressions for the time taken, horizontal distance covered, and fuel consumed during the fastest climb in standard atmosphere.

The basic relations of climb performance are discussed first and, thereafter, the expressions for airspeed, climb angle, and the rate of climb are reproduced.[1] These relations are used in this note to obtain analytical expressions for the endurance, range, and climb-fuel weight fraction during the fastest climb phase. The analysis is applied to a given aircraft and the results are presented graphically.

Received Sept. 8, 1991; revision received Nov. 9, 1991; accepted for publication Nov. 9, 1991.

*Professor, Department of Aerospace Engineering.

Basic Relations of Climb Performance

The important flight parameters of climb performance from altitude h_1 to h_2 are climb angle γ, rate of climb R/C, time taken in climb t, horizontal distance covered x, and the climb-fuel weight fraction ζ. These are obtained[1] for steady-state flight as

$$\gamma = \frac{T}{W} - \frac{1}{E}, \qquad R/C = \frac{T}{W}V - \frac{1}{E} \tag{1}$$

$$t = \int_{h_1}^{h_2} \frac{\mathrm{d}h}{R/C}, \qquad x = \int_{h_1}^{h_2} \frac{\mathrm{d}h}{\gamma} \tag{2}$$

$$\zeta = 1 - \exp\left(\int_{h_1}^{h_2} \frac{T/W}{R/C}\,\mathrm{d}h\right) \tag{3}$$

where C is considered constant. The fastest climb parameters are obtained with the help of the above relations.

Fastest Climb Parameters

The fastest climb airspeed, V_{FC}, is obtained by optimizing R/C of relation (1) with respect to V. This value of V when substituted in the expressions for γ and R/C, after expressing $1/E$ in terms of V, gives the climb angle γ_{FC}, and the rate of climb $(R/C)_{FC}$ of the fastest climb. The expressions have been developed by Hale[1] as

$$V_{FC} = \left[\frac{(T/W)(W/S)\Gamma}{3\rho_{SSL}\sigma C_{D0}}\right]^{1/2} \tag{4}$$

$$\gamma_{FC} = \frac{T}{W}\left(1 - \frac{\Gamma}{6}\right) - \frac{3}{2\Gamma E_m^2 (T/W)} \tag{5}$$

$$(R/C)_{FC} = \left(\frac{(W/S)\Gamma}{3\rho_{SSL}\sigma C_{D0}}\right)^{1/2}\left(\frac{T}{W}\right)^{3/2}\left(1 - \frac{\Gamma}{6}\right) \cdot \left\{1 - \frac{3}{2\Gamma\,[1 - (\Gamma/6)]E_m^2 (T/W)^2}\right\} \tag{6}$$

$$t_{FC} = \int_{h_1}^{h_2} \frac{\mathrm{d}h}{(R/C)_{FC}}, \qquad x_{FC} = \int_{h_1}^{h_2} \frac{\mathrm{d}h}{\gamma_{FC}} \tag{7}$$

$$\zeta_{FC} = 1 - \exp\left(-C\int_{h_1}^{h_2} \frac{(T/W)}{(R/C)_{FC}}\,\mathrm{d}h\right) \tag{8}$$

where

$$\Gamma = 1 + \sqrt{1 + [3/E_m^2 (T/W)^2]}$$
$$E_m = (1/2\sqrt{C_{D0}K}) \tag{9}$$

It has been pointed out by Hale that Γ lies between 2 and 3 only and therefore, he puts $\Gamma = 2$ as its constant value. Here we also consider Γ to be a constant but, to begin with, we do not assign any particular value to it.

Consider now that the fastest climb has taken place with constant throttle setting, we can approximate the thrust re-

quired variation with altitude (and thus σ) as

$$t = T_{SSL}\sigma \tag{10}$$

and for the sake of brevity, we now also introduce b as

$$b = \{(2/3)\Gamma[1 - (\Gamma/6)]\}^{1/2}E_m(T_{SSL}/W) \tag{11}$$

Equations (5) and (6) with the help of the above two relations can respectively be written as

$$\gamma_{FC} = \frac{T_{SSL}}{W}\left(1 - \frac{\Gamma}{6}\right)\left(\sigma - \frac{1}{b^2\sigma}\right) \tag{12}$$

$$(R/C)_{FC} = \left[\frac{(W/S)\Gamma}{3\rho_{SSL}C_{D0}}\right]^{1/2}\left(\frac{T_{SSL}}{W}\right)^{3/2}\left(1 - \frac{\Gamma}{6}\right)\left(\sigma - \frac{1}{b^2\sigma}\right) \tag{13}$$

The t_{FC}, x_{FC}, and ζ_{FC} as given in relations (7) and (8) become

$$t_{FC} = \left[\frac{3\rho_{SSL}C_{D0}}{(W/S)\Gamma}\right]^{1/2}\frac{1}{(T_{SSL}/W)^{3/2}[1 - (\Gamma/6)]} \cdot \int_{h_1}^{h_2}\frac{b^2\sigma}{b^2\sigma^2 - 1}\,dh \tag{14}$$

$$x_{FC} = \frac{1}{(T_{SSL}/W)[1 - (\Gamma/6)]}\int_{h_1}^{h_2}\frac{b^2\sigma^2}{b^2\sigma^2 - 1}\,dh \tag{15}$$

$$\zeta_{FC} = 1 - \exp\left\{-C\left[\frac{3\rho_{SSL}C_{D0}}{(T_{SSL}/W)(W/S)\Gamma}\right]^{1/2} \cdot \frac{1}{[1 - (\Gamma/6)]}\int_{h_1}^{h_2}\frac{b^2\sigma^2}{b^2\sigma^2 - 1}\,dh\right\} \tag{16}$$

where

$$\Gamma = 1 + \sqrt{1 + [3/E_m^2(T_{SSL}/W)^2\sigma^2]} \tag{17}$$

It is quite possible to assume in the above relations (14) to (16) that the wing loading (W/S) remains unchanged due to insignificant fuel consumption during the climb.

The density ratio σ can be connected[1] with the h as $\sigma = e^{-h/\beta}$, where $\beta = 9296$ m (30,500 ft) in troposphere and $\beta = 7254$ m (23,800 ft) in stratosphere. By introducing this value of σ, it is possible to evaluate the integrals in relations (14) to (16) and present them in analytical forms. We, therefore, obtain

$$t_{FC} = \left[\frac{3\rho_{SSL}C_{D0}}{(W/S)\Gamma}\right]^{1/2}\frac{1}{(T_{SSL}/W)[1 - (\Gamma/6)]}\frac{b\beta}{2} \cdot \ell_n\left[\frac{(be^{-h_2/\beta} - 1)(be^{-h_2/\beta} + 1)}{(be^{-h_1/\beta} + 1)(be^{-h_1/\beta} - 1)}\right] \tag{18}$$

$$x_{FC} = \frac{1}{(T_{SSL}/W)[1 - (\Gamma/6)]}\frac{b\beta}{2} \cdot \ell_n\left[\frac{(be^{-h_1/\beta} - 1)(be^{-h_2/\beta} + 1)}{(be^{-h_1/\beta} + 1)(be^{-h_2/\beta} - 1)}\right] \tag{19}$$

$$\zeta_{FC} = 1 - \exp\left\{\left[\frac{3\rho_{SSL}C_{D0}}{(T_{SSL}/W)(W/S)\Gamma}\right]^{1/2}\frac{C}{(1 - (\Gamma/6))} \cdot \frac{\beta}{2}\ell_n\left[\frac{(be^{-h_2/\beta} - 1)(be^{-h_2/\beta} + 1)}{(be^{-h_1/\beta} + 1)(be^{-h_1/\beta} - 1)}\right]\right\} \tag{20}$$

where Γ and b are given by relations (17) and (11), respectively.

Application to an Aircraft

A turbojet aircraft of wing loading 2873 N/m² (60 lb/ft²) and parabolic drag polar, $C_D = 0.02 + 0.057C_L^2$ is considered here. Its thrust-specific fuel consumption is 0.8/h. The two cases (0.3 and 0.2) of thrust-to-weight ratio at sea level are considered here. The climb is assumed steady with constant throttle setting in a standard atmosphere from sea level. We find here V_{FC}, γ_{FC}, $(R/C)_{FC}$, t_{FC}, x_{FC}, and ζ_{FC} at different altitudes in the region of trophosphere.

Therefore, $W/S = 2873$ N/m², $C_{D0} = 0.02$, $K = 0.057$, $E_m = 14.81$, and $C = 0.8/3600$/s. The standard atmospheric table gives $\rho_{SSL} = 1.226$ kg/m³. The climb is mostly considered in the trophosphere, therefore, $\beta = 9296$ m. Consider the two cases, $T_{SSL}/W = 0.3$ and $T_{SSL}/W = 0.2$. Since the climb takes place from the ground at sea level, $h_1 = 0$. Consider h_2 as variable by writing $h_2 = h$ that represents known altitude.

The V_{FC}, γ_{FC}, and $(R/C)_{FC}$ are obtained from Eqs. (4–6) respectively, and these are plotted against h in Fig. 1. The aircraft of lower T_{SSL}/W gives lower ceiling as shown by the horizontal dotted lines. The curves of t_{FC}, x_{FC} and ζ_{FC} are obtained from Eqs. (18–20) respectively, by assuming $\Gamma = 2.2$, and they are shown in Fig. 2. The aircraft of lower T_{SSL}/W takes a longer time, a larger distance, and higher fuel consumption to climb to a given altitude (provided the other design parameters of the aircraft are kept unaltered). The

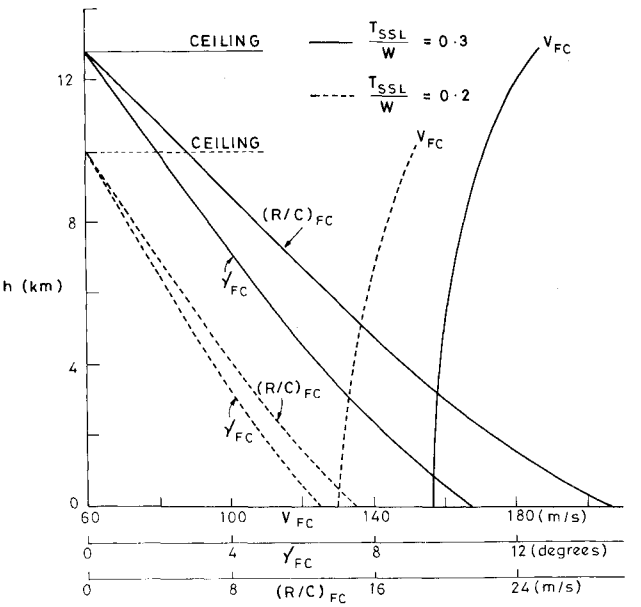

Fig. 1 Variations of V_{FC}, γ_{FC} and $(R/C)_{FC}$ with altitude.

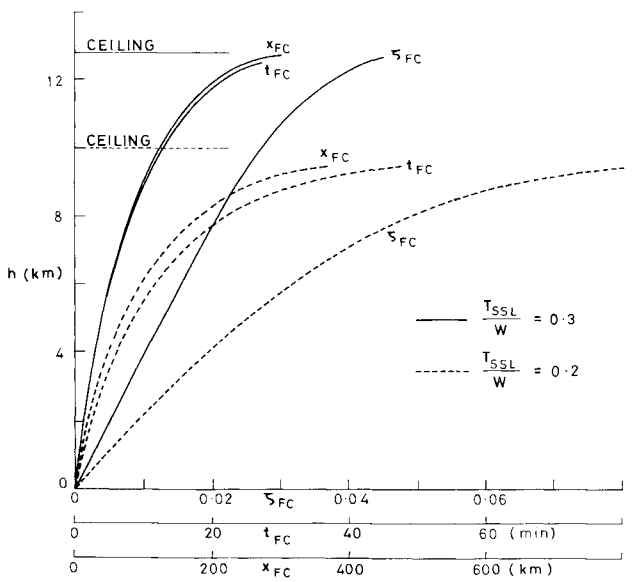

Fig. 2 Variations of x_{FC}, t_{FC} and ζ_{FC} with altitude.

behavior of these curves is the same as one generally finds in practice.

Reference

[1]Hale, F. J., "Aircraft Performance, Selection, and Design," 1st ed., Wiley, New York, 1984, pp. 42–54.

Nonunique Solutions in Unsteady Transonic Flow

H. S. Murty*
University of Ottawa, Ottawa, Ontario, Canada

Introduction

THE need to properly study the existence of nonunique solutions of the partial differential equations that govern transonic flowfields remains a problem in computational fluid dynamics. The need to determine whether these solutions are physically realizable, or are manifestations of the numerical modeling, is based on applications of these solutions. In particular, for unsteady flows, accurate dynamic load prediction is necessary for analysis and prediction of aeroelastic response.

Previously, several authors have commented on the causes of nonunique solutions in steady, small-disturbance, transonic flow models. Initially, Steinhoff and Jameson[1] pointed out the existence of nonuniqueness in steady, full potential flow solutions. They concluded from their steady-flow analysis, that the nonuniqueness appeared in a narrow band of freestream Mach numbers between 0.82–0.85. Since this Mach number band coincides with that in which buffet phenomena occur, a link was drawn between the presence of multiple solutions and real physical phenomena, and it was concluded that nonuniqueness was not merely a consequence of the numerical modeling.

An interesting comparison of the potential flow nonuniqueness phenomena with one-dimensional nozzle flow was suggested by Salas et al.[2] If the nozzle flow is choked, then what occurs in the divergent section is dependent on the downstream pressure. One possibility is a compression to subsonic flow. A second possibility is an isentropic compression at a supersonic speed. Otherwise, a shock wave could form in the divergent part of the nozzle with subsequent deceleration to subsonic flow. The authors suggest that the inability of the conservative potential equation to correctly position the shock wave, could be responsible for the nonuniqueness.

For unsteady flows, Williams, Bland, and Edwards[3] examined the nonuniqueness problem using a small-disturbance, potential flow model. The response of the NACA 00XX series of airfoils to a pitch pulse was examined. In this case, the airfoil undergoes a rapid increase in angle of attack, followed by a rapid decrease to the initial conditions. The flow responds to this sudden change, and then settles down in time, back to the initial steady flow conditions of zero lift. However, nonzero lift conditions were produced for the range of Mach numbers 0.835–0.858. They also noted that in this Mach number range, the shock waves formed between 72–88% chord. It is important to note that shock wave location is based on downstream pressure. The authors concluded, that because small-disturbance potential flow models and full potential flow models share the assumption of isentropic flow, the nonuniqueness would also occur in full potential flow models as well.

These same conclusions were noted by Fuglsang[4] who used the unsteady, transonic small disturbance code XTRAN2L[5] to carry out his computations. A NACA 0012 airfoil was subjected to a sudden change in angle of attack, at freestream Mach numbers between 0.82–0.85. The ensuing load distribution was determined as a function of time. As the pitch angle decayed in time, it was found that for a certain range of freestream Mach numbers, the lift coefficient did not decay to zero lift, thus indicating the presence of nonunique solutions.

The purpose of this work is to study the occurrence of nonunique solutions in unsteady transonic flows. In the present study, a full potential, unsteady code was developed and used. This code was applied to the analysis of flows past NACA 0012 and NACA 64A006 airfoils. Previous researchers[4,6] found nonunique solutions using transonic small disturbance (TSD) models. Our more accurate, full potential model, showed that these nonunique solutions do not actually exist in certain cases. These results are important in helping to determine the conditions under which nonunique solutions are possible in unsteady, computational flow models. To date, there has been no verification of nonunique solutions in unsteady flow, using either full potential or Euler codes. Details of the development and validation of the full potential code are given in Murty.[7]

Pitch Pulse Response

Fuglsang used XTRAN2L,[5] an unsteady small disturbance code, for all his computations. Starting from a steady-state solution, Fuglsang applied a pitch pulse

$$\alpha(t) = 0.00436 \exp[-0.0025(t - 100\Delta t)^2]$$

to the NACA 0012 airfoil. As the pitch angle decayed in time, for a certain range of Mach numbers, the lift coefficient did not decay to zero lift, thereby indicating the presence of nonunique solutions.

In the present study, the same test cases were carried out with the more accurate full potential unsteady code. These computations were carried out in the hope that the root cause of the nonuniqueness appearing from the small disturbance model, might become apparent. It was found that the lift coefficient does decay to zero as the pitch angle decays to zero (Fig. 1). All solutions converged to zero lift with the unsteady full potential code. If the cause of the nonuniqueness is the isentropic flow assumption in potential flow models, then the full potential flow model should also manifest the same property of nonuniqueness.

Considering the array of explanations given for the case of steady flow, a possible explanation for the difference between these small-disturbance and full potential flow results seems to appear from the accurate prediction of downstream pressure. The assumption of a thin body (inherent in the small disturbance code) assumes that the location of the wake to be on a coordinate line downstream of the airfoil. The full potential model, however, moves the wake location with the oscillation airfoil motion. The computational model still involves the assumption of the wake location to be on a coordinate line downstream of the airfoil. However, in this case, this coordinate line is in the computational domain. The transformation to Cartesian coordinates positions the wake on the trailing-edge bisector for symmetric airfoils. This difference in wake position location between small disturbance, and full potential flow models, may account for the difference in the presence of nonunique solutions by providing different down-

Received Oct. 27, 1991; accepted for publication Nov. 5, 1991.

*Research Associate. Member AIAA.